


Communication

# Bauerenol Acetate, the Pentacyclic Triterpenoid from *Tabernaemontana longipes*, is an Antitrypanosomal Agent

Simira Carothers <sup>1</sup>, Rogers Nyamwihura <sup>1</sup>, Jasmine Collins <sup>1</sup>, Huaisheng Zhang <sup>1</sup>,  
HaJeung Park <sup>2</sup>, William N. Setzer <sup>3</sup> and Ifedayo Victor Ogungbe <sup>1,\*</sup> 

<sup>1</sup> Department of Chemistry, Jackson State University, Jackson, MS 39217, USA; Simira.carothers@gmail.com (S.C.); rogersnyamwihura@yahoo.com (R.N.); Jcollins1908@gmail.com (J.C.); huiasheng.zhang@students.jsums.edu (H.Z.)

<sup>2</sup> X-ray Crystallography Laboratory, Scripps Research Institute-FL, Jupiter, FL 33458, USA; hajpark@scripps.edu

<sup>3</sup> Department of Chemistry, University of Alabama in Huntsville, Huntsville, AL 35899, USA; wsetzer@chemistry.uah.edu

\* Correspondence: ifedayo.v.ogungbe@jsums.edu; Tel.: +1-601-979-3719

Received: 21 December 2017; Accepted: 6 February 2018; Published: 8 February 2018

**Abstract:** The Latin American plant *Tabernaemontana longipes* was studied in this work as a potential source of antiparasitic agents. The chloroform extract of *T. longipes* leaves was separated into several fractions, and tested for antitrypanosomal activity. One of the fractions displayed significant growth inhibitory activity against *Trypanosoma brucei*. The active principle in the fraction was isolated, purified, and characterized by NMR and mass spectrometry. The antitrypanosomal agent in the CHCl<sub>3</sub> extract of *T. longipes* leaves is the pentacyclic triterpenoid bauerenol acetate. A metabolite profiling assay suggest that the triterpenoid influences cholesterol metabolism. The molecular target(s) of bauerenol and its acetate, like many other antiparasitic pentacyclic triterpenoids is/are unknown, but they present privileged structural scaffolds that can be explored for structure-based activity optimization studies using phenotypic assays.

**Keywords:** *Tabernaemontana longipes*; *Trypanosoma brucei*; trypanosomiasis; pentacyclic triterpenoid

## 1. Introduction

African sleeping sickness (Human African Trypanosomiasis) caused by protozoan *Trypanosoma brucei gambiense/rhodesiense* is still a public health problem in rural and remote regions of the continent, especially in the Democratic Republic of the Congo. Despite a gradual decrease in the number of reported cases in the past few years, the lack of effective and safe medicines, the unavailability of adequate and rapid diagnostic tools, especially in rural and remote places, and the possibility of continuous transmission of the parasite from animal reservoirs to humans, make the disease a continuous threat to millions of people [1–4]. To consolidate recent gains in the fight against the disease, continued integration of discovery and development of new drugs and new diagnostic tools with disease control and prevention strategies is of paramount importance. Therefore, discovery of new antitrypanosomal chemical entities using molecular target-based or phenotypic screening-based approaches remains very attractive.

In our on-going exploration of tropical plants as potential sources of new antitrypanosomal agents, *Tabernaemontana longipes* Donn. Sm. (Apocynaceae) was studied as a potential source of antitrypanosomal phytochemicals. *T. longipes* is a tropical plant found in several Latin American countries, including Nicaragua, Colombia, Ecuador, and Costa Rica. The plant's flowers are white or cream-colored, with cylindrical corollas and brown lobes, and the flowers smell sweet [5,6].

## 2. Results and Discussion

The leaves of *T. longipes* were obtained from several mature trees growing in Costa Rica in 2009. The leaves (1 kg) were dried, chopped, and extracted with refluxing chloroform for 6 h. The chloroform extract (14 g) was fractionated on silica gel (700 g) and eluted with 5:1 hexane/ethyl acetate mixture to obtain 49 fractions. The fractions were pooled together to obtain nine superfractions (SP1–9). The fractions were screened for their ability to inhibit the growth of *T. brucei* in vitro. SP2 displayed significant antitrypanosomal activity (76% growth inhibition at 10  $\mu\text{g}/\text{mL}$ ). SP2 (2.1 g) was subsequently separated using 10:1 hexane/ethyl acetate mixture over 200 g of silica gel to obtain seven fractions (SP2F1–SP2F7). The TLC profiles of the fractions showed that SP2F4 and SP2F5 have a major and similar component while the other fractions have several minor components. SP2F4 and SP2F5 were pooled together and purified by crystallization. SP2F4-5 (227 mg), a yellowish, oily amorphous solid, was dissolved in hexane and placed in a pentane tank for 24 h to induce crystallization. The resulting crystals were filtered, washed four times with pentane (2 mL), and allowed to dry, to give colorless needle-like crystals (1, 76 mg). The  $^1\text{H}$ - and  $^{13}\text{C}$ -NMR spectra of 1 suggested that it is a triterpenoid. The  $^{13}\text{C}$ -NMR spectrum shows 31 distinguishable carbon signals. The most characteristic structural features in the  $^{13}\text{C}$  spectrum include an ester carbonyl signal ( $\delta$  171.1) and an alkenyl carbon signal ( $\delta$  145.6). The  $^1\text{H}$  and HSQC spectra revealed that there are nine methyl groups, nine methylene groups, one alkenyl hydrogen, one oxygenated methine group, five non-oxygenated methine groups, and five quaternary carbons (Table 1 and Figure 1).

**Table 1.**  $^1\text{H}$ - and  $^{13}\text{C}$ -NMR Spectra Data for 1 and 2.

Position	1		2	
	$^{13}\text{C}$	$^1\text{H}$	$^{13}\text{C}$	$^1\text{H}$
1	36.6	1.18, 1.66 (2H, m)	37.02	1.09, 1.64 (2H, m)
2	24.3	1.66 (2H, m)	27.8	1.61 (2H, m)
3	81.3	4.51 (1H, dd)	79.4	3.24 (1H, dd)
4	37.9		39.0	
5	48.3	2.21 (1H, m)	48.3	2.19 (1H, m)
6	24.1	1.97, 2.14 (2H, m)	24.3	1.97, 2.16 (2H, m)
7	116.4	5.40 (1H, m)	116.5	5.41 (1H, m)
8	145.6		145.4	
9	50.7	1.41 (1H, m)	50.5	1.29 (1H, m)
10	35.0		35.3	
11	32.5	1.48, 1.56 (2H, m)	32.5	1.48, 1.54 (2H, m)
12	31.6	1.14, 1.61 (2H, m)	31.6	1.14, 1.60 (2H, m)
13	37.8		37.86	
14	37.9		37.86	
15	28.8	1.40, 1.50 (2H, m)	29.0	1.41, 1.49 (2H, m)
16	16.7	1.48, 1.54 (2H, m)	16.9	1.48, 1.54 (2H, m)
17	41.2		41.3	
18	55.0	1.29 (1H, s)	55.0	1.29 (1H, s)
19	35.3	1.15 (1H, m)	35.4	1.14 (1H, m)
20	31.8	1.54 (1H, m)	31.8	1.54 (1H, m)
21	29.3	1.19, 1.51 (2H, m)	29.3	1.19, 1.51 (2H, m)
22	37.8	1.18, 1.48 (2H, m)	37.82	1.18, 1.49 (2H, m)
23	15.9	0.93 (3H, s)	14.8	0.85 (3H, s)
24	27.6	0.85 (3H, s)	27.6	0.96 (3H, s)
25	13.1	0.76 (3H, s)	13.1	0.74 (3H, s)
26	23.6	0.99 (3H, s)	23.8	0.99 (3H, s)
27	22.8	0.94 (3H, s)	22.8	0.94 (3H, s)
28	37.9	1.02 (3H, s)	38.1	1.02 (3H, s)
29	25.8	1.04 (3H, d)	25.8	1.04 (3H, d)
30	22.6	0.90 (3H, d)	22.7	0.90 (3H, d)
OAc	21.4, 171.1	2.05 (3H, s)		

The connectivity of the carbon-carbon atoms, and their hydrogen atoms was deciphered using a combination of HMBC, COSY, and HSQC data (Table 1 and Figure S1 in Supplementary File 1). The HMBC data provide a clear correlation between one of the methyl groups and the carbonyl carbon that is typical of acetylated triterpenoid, while the carbon connectivity suggested that is a pentacyclic triterpenoid [7]. The relative stereochemistry of the compound was established by nuclear Overhauser effect (NOE) correlations, and X-ray diffraction data from a single plate crystal.

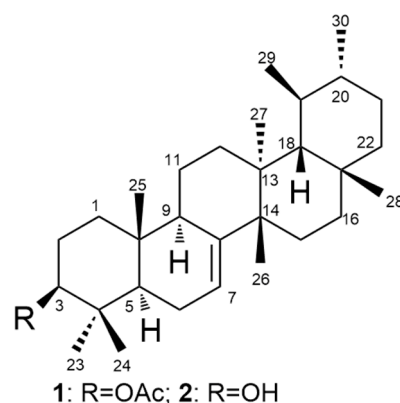


**Figure 1.** Structure of compounds 1 and 2.

Its molecular formula,  $C_{32}H_{52}O_2$ , was established from high resolution mass spectrometry (HRMS; TOFMS ESI+,  $[M + Li]^+$   $m/z$  475.4113, for  $C_{32}H_{52}O_2Li$ , Figure S2), and CH elemental analysis (Found: C = 81.37% and H = 11.13%; Calculated: C = 81.99% and H = 11.18%). The compound (**1**) was identified as bauerenol acetate, a pentacyclic triterpenoid that had been previously identified in *Tabernaemontana longipes* [8,9]. Compound **1** was then tested for its ability to inhibit the growth of *T. brucei* in vitro. The results showed that bauerenol acetate has an  $IC_{50}$  value of 3.1  $\mu M$  (Table 2).

**Table 2.** Bioassay data of compounds 1 and 2.

Compound	<i>T. brucei</i> Growth Inhibition $IC_{50}$ ( $\mu M$ )	Cytotoxicity Hep G2 $IC_{50}$ ( $\mu M$ )
<b>1</b>	3.09 $\pm$ 0.80	>80
<b>2</b>	2.71 $\pm$ 0.96	>80
Suramin	0.04 $\pm$ 0.01	n/a

Due to the relatively poor solubility of the acetate in DMSO during the bioassay, the acetate was subjected to hydrolysis in 5% ethanolic KOH to obtain its alcohol derivative bauerenol (**2**). The solubility of bauerenol in DMSO was somewhat better than the acetate, and its activity on *T. brucei* in vitro was characterized by an  $IC_{50}$  value of 2.7  $\mu M$ . The antitrypanosomal activities of these compounds are much lower (1–3 order of magnitude) than clinically used antitrypanosomal drugs [10]. Also, the  $IC_{50}$  values of **1** and **2** are higher than the  $IC_{50}$  value (<1  $\mu M$ ) proposed by Nwaka and Hudson as criteria for preclinical evaluation of antitrypanosomal drug candidates [11]. A number of oleanolic and ursolic acid-based pentacyclic triterpenoids have previously reported to have growth inhibitory activity against *Leishmania* spp. and *T. cruzi* but not *T. brucei* [12–17].

Several pentacyclic triterpenoids have been shown to be cytotoxic or described as potential anticancer agents [18–20]. Therefore, we decided to test if **1** and **2** are cytotoxic to human hepatocarcinoma cell model (Hep G2) or if they show selective antitrypanosomal activity. Both compounds have very little effect on cellular viability on Hep G2 cells ( $IC_{50}$  > 80  $\mu M$ ). The molecular target (macromolecule or pathway) of these compounds is yet to be experimentally determined and could be the subject of future studies, but previous docking studies have suggested *T. brucei* sterol 14 $\alpha$ -demethylase to be a potential target for triterpenoids [21].

Nevertheless, to understand how the pentacyclic triterpenoid (**2**) affect *T. brucei* cells, a primary metabolite profiling assay was carried out. The metabolites were identified and quantified using GC-TOFMS as outlined in the methods section below. A total of 90 metabolites were unambiguously identified and quantified (Supplementary File 2) in the assay. The metabolites with the most notable concentration-dependent changes in the parasites are stearic acid, phosphoenolpyruvate, myristic acid, cholesterol, arachidic acid, and adenine. The changes in the levels of cholesterol were the most consistent and conceivably the most informative from the metabolite profiling assay. The levels of cholesterol (Figures 2 and S3) in parasites treated with 5  $\mu$ M of **2** was significantly increased when compared to the control group ( $n = 6$ ,  $p$ -value = 0.0023) and the group treated with 0.15  $\mu$ M of **2** ( $n = 6$ ,  $p$ -value = 0.0072). This suggests that the triterpenoid is interfering with the metabolism of endogenous sterol(s) or a cholesterol-dependent pathway. Previous studies have shown that accumulation of cholesterol by trypanosomes is associated with perturbation of the endogenous sterol biosynthetic pathway [22–25]. Therefore, sterol biosynthetic pathway in *T. brucei* is the likely target of bauerenol (**2**).

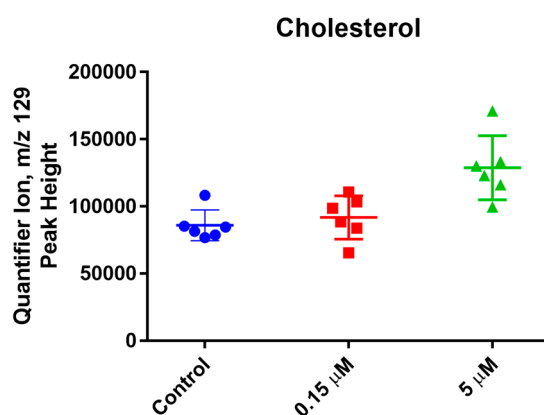


**Figure 2.** Levels of cholesterol in parasite treated with bauerenol (**2**). The levels of cholesterol in the parasite was significantly increased after 4-h exposure to 5  $\mu$ M of **2**.

In conclusion, bauerenol and its acetate are anti-*T. brucei* agents. The structure of bauerenol (**2**) can be used as a starting structural motif in natural products-based diversity oriented synthesis (DOS) or in the synthesis of derivatives that have better drug-like physicochemical properties. Further studies are necessary to determine the specific enzyme or metabolic step directly affected by bauerenol.

### 3. Materials and Methods

#### 3.1. Plant Material

*T. longipes* leaves were collected in May 2009, in the Monteverde region of northwestern Costa Rica (10°18'3.4'' N, 84°48'39.3'' W, 1381 m elevation). The plant was identified by William A. Haber. A voucher specimen has been deposited with the Missouri Botanical Garden herbarium (Haber Collection No. 7104).

#### 3.2. Compound Characterization

All chromatographic separations were carried out on Sortech's silica gel (Premium Rf, 60 Å, 40–75  $\mu$ m). The 1D ( $^1\text{H}$  and  $^{13}\text{C}$ ) and 2D (gCOSY, gHSQC, gHMBC, NOESY) data were collected on a 500 MHz (13C: 125 MHz) Varian INOVA spectrometer operated with *Vnmrj*. Chloroform- $d$  was used as solvent, and tetramethylsilane (TMS) as internal standard in the solvent. The mass spectra were obtained on a Synapt G2 HDMS instrument (Waters; Milford, MA, USA) operated in positive ESI mode. Elemental analysis was carried out on a Costech's ECS 4010 (Valencia, CA, USA). The infrared spectra were obtained on a Perkin Elmer Spectrum 100 FT-IR spectrometer (Waltham, MA, USA) using

an ATR accessory. Please see Figures S1, S2 and S4–S7 in Supplementary File 1 for NMR, IR, Anal, and MS spectra as well as the crystal structure.

Crystals of **1** were obtained by slow evaporation of a chloroform solution of **1**. X-ray diffraction data were collected on a Bruker AXS Smart APEX CCD II [Mo K $\alpha$  ( $\lambda = 0.71073$  Å)] (Madison, WI, USA) at 295 K. The structure was solved by Olex2 using SHELXTL and was refined by full-matrix least-squares procedure (Figure S6) Non-hydrogen atoms were refined anisotropically. Hydrogen atoms were added in calculated positions and were refined. Melting points were recorded on a MEL-TEMP 1101D apparatus (Dubuque, IA, USA). The melting point values are uncorrected.

### 3.2.1. Bauerenol Acetate (**1**)

Colorless crystals; melting point 289–291 °C; IR (CHCl<sub>3</sub>)  $\nu_{\max}$  2935, 1732, 1463, 1374, 1249, 1026 cm<sup>-1</sup>; <sup>1</sup>H- and <sup>13</sup>C-NMR, see Table 1; HRMS ESI+ [(M + Li)<sup>+</sup>],  $m/z$  475.4113 [Calculated for C<sub>32</sub>H<sub>52</sub>O<sub>2</sub>Li 475.4128].

### 3.2.2. Bauerenol (**2**)

Colorless solid; melting point 202–203 °C; IR (CHCl<sub>3</sub>)  $\nu_{\max}$  3379, 2929, 2866, 1457, 1372, 1032 cm<sup>-1</sup>; <sup>1</sup>H- and <sup>13</sup>C-NMR, see Table 1; HRMS ESI+ [(M + H)<sup>+</sup>],  $m/z$  427.3922 [Calculated for C<sub>30</sub>H<sub>51</sub>O<sub>2</sub> 427.3940].

## 3.3. Trypanosoma brucei Assay

The growth inhibitory activity of the compounds was evaluated using the Alamar blue assay [26]. Bloodstream form of *T. brucei* (strain 427) cultured in HMI-9-medium supplemented with 10% FBS, 10% Serum plus (SAFC), 0.05 mM bathocuproine sulfonate, 1.5 mM L-cysteine, 1 mM hypoxanthine, 0.2 mM  $\beta$ -mercaptoethanol, 0.16 mM thymidine, 1 mM pyruvate, and 0.0125% Tween 80 was used. Parasites were dispensed into a sterile 96-well plate at  $5 \times 10^3$  cells/well and treated with compound **1** and **2** for 24 h. The compounds were prepared in DMSO containing 1.25% Tween 80. Final concentration of Tween 80 in the assay wells was 0.0125%. The compounds were screened in triplicate with a total assay volume of 100  $\mu$ L. Next, Alamar blue (20  $\mu$ L) was added and the plate was incubated at 37 °C for 4 h. Immediately following incubation, fluorescence signals were read ( $\lambda_{\text{ex}}$  530 nm,  $\lambda_{\text{em}}$  590 nm). Suramin was used as positive control.

## 3.4. Cytotoxicity Assay

Human hepatocarcinoma cell line (Hep G2 CRL-11997<sup>TM</sup>, ATCC) was used for cytotoxicity studies. The cells were grown in complete medium (DMEM: F12 containing L-glutamine and sodium bicarbonate, 10% FBS, 1% penicillin/streptomycin, 0.0125% Tween 80) incubated at 37 °C in a 5% CO<sub>2</sub> environment. Once 80–90% confluent, the cells were washed with phosphate-buffered saline (PBS), treated with 0.25% ( $w/v$ ) of trypsin/EDTA, counted and suspended in fresh complete media. Into 96-well plates,  $5 \times 10^5$  cells/mL were seeded and incubated for 24 h. Cells were treated with the compounds prepared in DMSO containing 1.25% Tween 80 for 72 h. Final concentration of Tween 80 in the assay wells was 0.0125%. Thereafter, DMEM:F12 medium containing MTT (5 mg/mL in PBS) was added to the cells and incubated for 1 h. The MTT-containing medium was then gently removed and replaced with DMSO (200  $\mu$ L/well), the plate was then mixed gently to allow the formazan crystals to dissolve. Absorbance was measured at 550 nm. All compounds were tested in triplicates. SDS (10%) was used as positive control.

## 3.5. Metabolic Profiling

*T. brucei* cells in supplemented HMI-9 medium were treated with 5  $\mu$ M and 0.15  $\mu$ M of **2** for 4 h. After treatment, the cells were washed three times with PBS, and the cell pellets were stored at –80 °C for subsequent GC-MS analysis. The treatment was carried in sextuplicate, including six no

treatment controls. Ten million cells per replicate were used. Metabolites were extracted from the cells by adding 0.5 mL of 3:3:2 acetonitrile:isopropanol:water mixture to each sample followed by the addition of 3 stainless steel grinding beads and then transferred to a GenoGrinder (Metuchen, NJ, USA) for grinding. The cells were grinded for 30 s at 1500 rpm, and centrifuged at  $14,000 \times g$  for 5 min. The supernatants were transferred to new tubes. The extraction was repeated twice, and the pooled supernatant was concentrated to 500  $\mu$ L. The samples were silylated using MSTFA + 1% TMCS at 37 °C, and were used for primary metabolite profiling on a LECO Pegasus IV GC-time of flight mass spectrometer (Saint Joseph, MI, USA) as described by Fiehn and co-workers [25]. The GC-TOFMS analysis was carried out at the NIH West Coast Metabolomics Center at the University of California, Davis.

The samples (0.5  $\mu$ L each) were analyzed using the splitless mode on a Rtx-5Sil MS capillary column (30 m length  $\times$  0.25 mm internal diameter with 0.25  $\mu$ m film made of 95% dimethyl/5% diphenylpolysiloxane, Restek Corporation, Bellefonte, PA, USA). The gas flow-rate was 1 mL/min. Initial injection temperature was set at 50 °C and ramped up to 250 °C at a rate of 12 °C/s. Initial oven temperature was set at 50 °C for 1 min, then ramped up to 330 °C at a rate of 20 °C/min, and held constant for 5 min. The TOF mass spectrometer (LECO; Saint Joseph, MI, USA) unit mass resolution was set at 17 spectra/s from 80–500 Da at  $-70$  eV ionization energy and 1800 V detector voltage. The transfer line and the ion source temperatures were set at 230 °C and 250 °C, respectively. The primary metabolites were identified and quantified using the quantifier ions shown in Supplementary File 2. The raw mass spectra for the metabolites were processed by BinBase (BB) software (FiehnLab; Davis, CA, USA). The relative quantification was carried out using the peak height of each quantifier ion. The peak heights were normalized by dividing them by the sum of all peak heights for all identified metabolites and multiplied by the average peak heights for all identified metabolites in each sample [27,28].

**Supplementary Materials:** The NMR, IR, CH elemental analysis, and MS spectra as well as the GC-TOFMS Data are provided as supplementary material. Supplementary materials are available online.

**Acknowledgments:** This work was carried out in part by resources made available by the US National Institutes of Health (SC2GM109782, SC3GM122629, and G12MD007581). SC was supported by NSF-LSAMP Bridge to the Doctorate (HRD-1500317). We thank William Haber for plant identification. We are grateful to the Monteverde Cloud Forest Preserve and the Tropical Science Center for permission to collect plant materials under a cooperative rights agreement and to the Commission for the Development of Biodiversity of Costa Rica's Ministry of the Environment, Energy, and Telecommunications for Research Permit R-001-2006-OT-CONAGEBIO. This work was performed as part of the activities of the Research Network Natural Products against Neglected Diseases (ResNet-NPND), <http://www.resnetnpnd.org>.

**Author Contributions:** Simira Carothers, William N. Setzer, and Ifedayo Victor Ogungbe conceived and designed the experiments; Simira Carothers, Jasmine Collins, Rogers Nyamwihura, Huaisheng Zhang, HaJeung Park, William N. Setzer, and Ifedayo Victor Ogungbe performed the experiments; Simira Carothers, Jasmine Collins, HaJeung Park, and Ifedayo Victor Ogungbe analyzed the data; Ifedayo Victor Ogungbe and William N. Setzer contributed reagents/materials/analysis tools; Ifedayo Victor Ogungbe wrote the paper, and the paper was reviewed by all authors.

**Conflicts of Interest:** The authors declare no conflict of interest. The sponsors had no role in the design of the study; in the collection, analyses, or interpretation of data; in the writing of the manuscript, or in the decision to publish the results.

## References

1. Büscher, P.; Cecchi, G.; Jamonneau, V.; Priotto, G. Human African trypanosomiasis. *Lancet* **2017**, *390*, 2397–2409. [[CrossRef](#)]
2. Franco, J.R.; Simarro, P.P.; Diarra, A.; Jannin, J.G. Epidemiology of human African trypanosomiasis. *Clin. Epidemiol.* **2014**, *6*, 257–275. [[PubMed](#)]
3. Steverding, D. The history of African trypanosomiasis. *Parasites Vectors.* **2008**, *1*, 3. [[CrossRef](#)] [[PubMed](#)]
4. Lumbala, C.; Simarro, P.P.; Cecchi, G.; Paone, M.; Franco, J.R.; Kande Betu Ku Mesu, V.; Makabuza, J.; Diarra, A.; Chansy, S.; Priotto, G.; et al. Human African trypanosomiasis in the Democratic Republic of the Congo: Disease distribution and risk. *Int. J. Health Geogr.* **2015**, *14*. [[CrossRef](#)] [[PubMed](#)]



5. Smith, J.D. Undescribed plants from Guatemala and other Central American republics. *Bot. Gaz.* **1897**, *24*, 389–398. [[CrossRef](#)]
6. Morales, J.F. Estudios en las Apocynaceae Neotropicales XV: Sinopsis del género *Thoreaua* (Apocynoideae, Echteae), con una nueva especie de Veracruz, México. *Brittonia* **2005**, *57*, 258–263. [[CrossRef](#)]
7. Mahato, S.B.; Kundu, A.P. <sup>13</sup>C NMR spectra of pentacyclic triterpenoids—A compilation and some salient features. *Phytochemistry* **1994**, *37*, 1517–1575. [[CrossRef](#)]
8. Ciccío, J.; Hoet, P. Algunos constituyentes de los frutos y de las hojas de *Tabernaemontana longipes* Donn. Smith. *Rev. Latinoam. Quim.* **1981**, *12*, 88–90.
9. Tinant, B.; Germain, G.; Declercq, J.P.; van Meerssche, M.; Ciccío, J.F.; Hoet, P. Crystal structure of baurenyl acetate from *Tabernaemontana longipes* Donn. Smith. *Bull. Soc. Chim. Belg* **2010**, *91*, 117–121. [[CrossRef](#)]
10. Steverding, D. Evaluation of trypanocidal activity of combinations of anti-sleeping sickness drugs with cysteine protease inhibitors. *Exp. Parasitol.* **2015**, *151*, 28–33. [[CrossRef](#)] [[PubMed](#)]
11. Nwaka, S.; Hudson, A. Innovative lead discovery strategies for tropical diseases. *Nat. Rev. Drug Discov.* **2006**, *5*, 941–955. [[CrossRef](#)] [[PubMed](#)]
12. Peixoto, J.A.; Andrade e Silva, M.L.; Crotti, A.E.M.; Cassio Sola Veneziani, R.; Gimenez, V.M.M.; Januário, A.H.; Groppo, M.; Magalhães, L.G.; Dos Santos, F.F.; Albuquerque, S.; et al. Antileishmanial activity of the hydroalcoholic extract of *Miconia langsdorffii*, isolated compounds, and semi-synthetic derivatives. *Molecules* **2011**, *16*, 1825–1833. [[CrossRef](#)] [[PubMed](#)]
13. Leite, J.P.V.; Oliveira, A.B.; Lombardi, J.A.; Filho, J.D.S.; Chiari, E. Trypanocidal activity of triterpenes from *Arrabidaea triplinervia* and derivatives. *Biol. Pharm. Bull.* **2006**, *29*, 2307–2309. [[CrossRef](#)] [[PubMed](#)]
14. Cunha, W.R.; Crevelin, E.J.; Arantes, G.M.; Crotti, A.E.M.; Silva, M.L.A.E.; Furtado, N.A.J.C.; Albuquerque, S.; da Ferreira, D.S. A study of the trypanocidal activity of triterpene acids isolated from *Miconia* species. *Phytother. Res.* **2006**, *20*, 474–478. [[CrossRef](#)] [[PubMed](#)]
15. Del Rayo Camacho, M.; Mata, R.; Castaneda, P.; Kirby, G.C.; Warhurst, D.C.; Croft, S.L.; Phillipson, J.D. Bioactive compounds from *Celaenodendron mexicanum*. *Planta Med.* **2000**, *66*, 463–468. [[CrossRef](#)]
16. Cunha, W.R.; Martins, C.; Ferreira, D.S.; Crotti, A.E.M.; Lopes, N.P.; Albuquerque, S. In vitro trypanocidal activity of triterpenes from *Miconia* species. *Planta Med.* **2003**, *69*, 470–472. [[PubMed](#)]
17. Domínguez-Carmona, D.B.; Escalante-Erosa, F.; García-Sosa, K.; Ruiz-Pinell, G.; Gutierrez-Yapu, D.; Chan-Bacab, M.J.; Giménez-Turba, A.; Peña-Rodríguez, L.M. Antiprotozoal activity of Betulinic acid derivatives. *Phytomedicine* **2010**, *17*, 379–382. [[CrossRef](#)] [[PubMed](#)]
18. Chudzik, M.; Korzonek-Szlacheta, I.; Król, W. Triterpenes as potentially cytotoxic compounds. *Molecules* **2015**, *20*, 1610–1625. [[CrossRef](#)] [[PubMed](#)]
19. Laszczyk, M. Pentacyclic triterpenes of the lupane, oleanane and ursane group as tools in cancer therapy. *Planta Med.* **2009**, *75*, 1549–1560. [[CrossRef](#)] [[PubMed](#)]
20. Salvador, J.A.R.; Moreira, V.M.; Gonçalves, B.M.F.; Leal, A.S.; Jing, Y. Ursane-type pentacyclic triterpenoids as useful platforms to discover anticancer drugs. *Nat. Prod. Rep.* **2012**, *29*, 1463. [[CrossRef](#)] [[PubMed](#)]
21. Setzer, W.N.; Ogungbe, I.V. In-silico investigation of antitrypanosomal phytochemicals from Nigerian medicinal plants. *PLoS Neglect. Trop. D* **2012**, *6*, e1727. [[CrossRef](#)] [[PubMed](#)]
22. Urbina, J.A.; Vivas, J.; Visbal, G.; Contreras, L.M. Modification of the sterol composition of *Trypanosoma (Schizotrypanum) cruzi* epimastigotes by  $\Delta 24$  (25)-sterol methyl transferase inhibitors and their combinations with ketoconazole. *Mol. Biochem. Parasitol.* **1995**, *73*, 199–210. [[CrossRef](#)]
23. Urbina, J.A.; Vivas, J.; Lazard, K.; Molina, J.; Payares, G.; Pirns, M.M.; Piras, R. Antiproliferative effects OF  $\Delta 24$  (25) sterol methyl transferase inhibitors on *Trypanosoma (Schizotrypanum) cruzi*: In vitro and in vivo Studies. *Chemotherapy* **1996**, *42*, 294–307. [[CrossRef](#)] [[PubMed](#)]
24. Sharma, A.I.; Olson, C.L.; Mamede, J.I.; Gazos-Lopes, F.; Epting, C.L.; Almeida, I.C.; Engman, D.M. Sterol targeting drugs reveal life cycle stage-specific differences in trypanosome lipid rafts. *Sci. Rep.* **2017**, *7*, 9105. [[CrossRef](#)] [[PubMed](#)]
25. Gros, L.; Castillo-Acosta, V.M.; Jiménez, C.J.; Sealey-Cardona, M.; Vargas, S.; Estévez, A.M.; Yardley, V.; Rattray, L.; Croft, S.L.; Ruiz-Perez, L.M.; et al. New azasterols against *Trypanosoma brucei*: Role of 24-sterol methyltransferase in inhibitor action. *Antimicrob. Agents Chemother.* **2006**, *50*, 2595–2601. [[CrossRef](#)] [[PubMed](#)]
26. Ráz, B.; Iten, M.; Grether-Bühler, Y.; Kaminsky, R.; Brun, R. The Alamar Blue<sup>®</sup> assay to determine drug sensitivity of African trypanosomes (*T. b. rhodesiense* and *T. b. gambiense*) in vitro. *Acta Trop.* **1997**, *68*, 139–147.

27. Fiehn, O.; Wohlgemuth, G.; Scholz, M.; Kind, T.; Lee, D.Y.; Lu, Y.; Moon, S.; Nikolau, B. Quality control for plant metabolomics: Reporting MSI-compliant studies. *Plant J.* **2008**, *53*, 691–704. [[CrossRef](#)] [[PubMed](#)]
28. Aguer, C.; Piccolo, B.D.; Fiehn, O.; Adams, S.H.; Harper, M.E. A novel amino acid and metabolomics signature in mice overexpressing muscle uncoupling protein 3. *FASEB J.* **2017**, *31*, 814–827. [[CrossRef](#)] [[PubMed](#)]

**Sample Availability:** Samples of the compounds are available from the authors.



© 2018 by the authors. Licensee MDPI, Basel, Switzerland. This article is an open access article distributed under the terms and conditions of the Creative Commons Attribution (CC BY) license (<http://creativecommons.org/licenses/by/4.0/>).